Journal of
Water & Climate Change

IWA PUBLISHING

Journal of Water and Climate Change Vol 14 No 7, 2323 doi: 10.2166/wcc.2023.062

Evaluating the impact of projected CO_2, temperature, and rainfall change on groundwater resources in a rice–wheat dominated cropping region of northwestern India

Satyendra Kumar[a], Viveka Nand[b], Bhaskar Narjary[a,*], Pavan Kumar Harode[a], Adlul Islam[c], R. K. Yadav[a] and S. K. Kamra[a]

[a] ICAR-Soil Salinity Research Institute, Karnal 132001, India
[b] Department of Bio-Resource Engineering, McGill University, 21111 Lakeshore Road, Ste-Anne-de-Bellevue, QC H9X 3V9, Canada
[c] NRM Division (ICAR), KAB II, New Delhi 110012, India
*Corresponding author. E-mail: bhaskar.narjary@icar.gov.in

BN, 0000-0002-3148-2204

ABSTRACT

Increasing CO_2 concentration, temperature rise, and changes in rainfall due to climate change are expected to influence groundwater resources in irrigated agricultural regions. A simulation study using AquaCrop and MODFLOW models was undertaken to assess the combined effects of increasing CO_2 concentrations, temperature, and rainfall changes on groundwater behavior in a rice–wheat cropping region of northwest India. Simulations were carried out for the 2016–2099 period under two scenarios: increasing CO_2 concentrations corresponding to different RCPs (Scenario-I) and at a constant CO_2 concentration of 369.4 ppm (Scenario-II). The results indicate that elevated CO_2 negates the effect of rising temperature on evapotranspiration (ET) and water demand, and thus, lower ET is simulated under Scenario-I than Scenario-II for different RCPs during the future periods. The lower projected ET resulted in lower rice (2.3%–6.3%) and wheat (1.4%–16.1%) irrigation demand under Scenario-I than under Scenario-II. Of all RCPs, the lowest groundwater level (GWL) decline of 9.2, 20.5, and 24.4 m from the reference GWL (18.85 m) at the end of the early, mid-, and end-century periods, respectively, is projected under RCP8.5 and Scenario-I. Simulation results indicate that CO_2 concentration plays an important role while assessing climate change effects on groundwater in irrigated agricultural systems.

Key words: AquaCrop, climate change, CO_2 concentration, crop evapotranspiration, groundwater level, irrigation requirement

HIGHLIGHTS

- Quantified crop water budgeting components and their effect on groundwater levels in response to elevated CO_2 concentration.
- Rice irrigation requirement (IR) would decrease slightly while wheat IR significantly increased in future periods both in elevated CO_2 and constant CO_2 concentration scenarios.
- Groundwater level is projected to decline less in elevated CO_2 than in constant CO_2 concentration scenario.

GRAPHICAL ABSTRACT

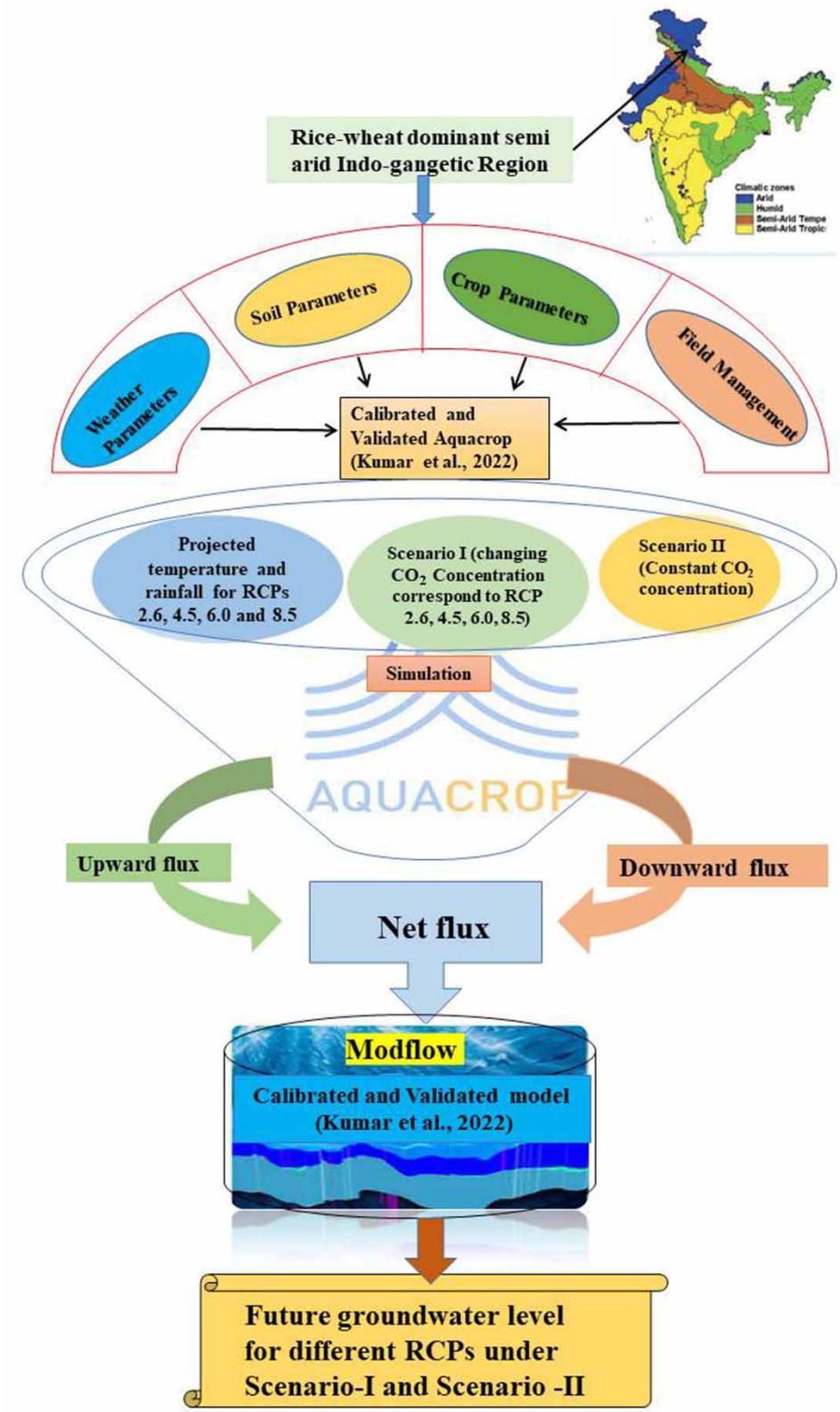

1. INTRODUCTION

In the past few decades, alteration in climatic parameters due to global warming has affected the availability of surface and groundwater resources worldwide, particularly in water-scarce arid and semi-arid regions. For instance, in the northwest Indo-Gangetic plains of India, high water-consuming rice–wheat crop rotation with inadequate canal water supply has resulted in an alarming decline in groundwater levels (Ministry of Agriculture – MOA 2013). Since the emission of greenhouse gases (carbon dioxide (CO_2), methane (CH_4), nitrous oxide (N_2O), and others) is increasing due to industrialization and changing human lifestyle, rise in temperature and changed precipitation patterns are directly or indirectly influencing local and regional hydrological and agricultural ecosystems. Under the representative concentration pathways (RCPs), the global average temperature is projected to increase by 1.7, 2.6, 3.1, and 4.8 °C under RCP2.6, RCP4.5, RCP6.0, and RCP8.5, respectively (IPCC 2013). The atmospheric CO_2 concentration is projected to increase to 430, 530, 670, and 936 ppm from the base level of 330 ppm under RCP2.6, RCP4.5, RCP6.0, and RCP8.5, respectively, by the end of the 21st century (IPCC 2013).

While the increase in air temperature leads to a direct rise in evaporation (Nand *et al.* 2021), the CO_2 concentration influences plant transpiration in two ways: diminishing of stomatal conductance with a decrease of stomatal opening (Hong *et al.* 2019; Bhargava & Mitra 2021) and a rise in leaf area index (LAI) and cell expansion leading to enhanced crop water requirement during the early growing period (Ficklin *et al.* 2010; Kirschbaum & McMillan 2018). Morison (1987) reported a 40% linear reduction in leaf stomatal opening with the doubling of CO_2 concentration from 330 to 660 ppm. Similarly, elevated CO_2 concentration resulted in an increase in LAI and biomass (Mndela *et al.* 2022), a reduction in transpiration rate and a consequent increase in water use efficiency (Eamus 1991; Field *et al.* 1995; O'Grady *et al.* 2011; Islam *et al.* 2012b; Hatfield & Dold 2019), reduction in crop evapotranspiration (Islam *et al.* 2012a, 2012b; Priya *et al.* 2014), increase in global mean runoff, and decrease in groundwater recharge (Ficklin *et al.* 2010; Andaryani *et al.* 2022). Reinecke *et al.* (2021) reported large uncertainties in modeling groundwater recharge as projected changes strongly vary among the different global hydrological models (GHMs)–global circulation models (GCMs) combinations due to the complicated process feedbacks between vegetation and water (transpiration changes due to available water together with vegetation productivity) and complex feedbacks between changes in CO_2, temperature, and precipitation which affect vegetation. In other words, the projected increase in CO_2 concentration under different climate change scenarios is likely to influence crop evapotranspiration, irrigation requirement, groundwater recharge, and groundwater extraction in agriculturally dominant regions.

Although the impacts of climate change on evapotranspiration, irrigation requirements, water footprints, and groundwater draft have been studied in India (Chattaraj *et al.* 2014; Abeysingha *et al.* 2016; Kambale *et al.* 2016; Dar *et al.* 2017; Mali *et al.* 2021), the interaction of atmospheric CO_2 concentration with different climate and crop parameters has not been accounted for. Furthermore while, the integrated impact of increasing levels of temperature and CO_2 concentrations on crop evapotranspiration, water use efficiency, and crop yield has been assessed (Jalota *et al.* 2009; Priya *et al.* 2014; Mohanty *et al.* 2015; Pandey *et al.* 2017; Lenka *et al.* 2020), the combined effect of elevated CO_2 and climate change on water budget components including groundwater behavior has not been studied. Kumar *et al.* (2022) modeled the impact of climate change on groundwater and adaptation strategies for its sustainable management for the Karnal district of the northwestern region of India, but the interaction of projected CO_2 concentrations with the anticipated changes in temperature and rainfall was not accounted for. It is hypothesized that elevated atmospheric CO_2 concentration levels under changing rainfall and air temperature regimes of different climate change scenarios would influence water budget components and consequently groundwater extraction and water table in a groundwater irrigated region.

Groundwater flow models are commonly used to study complex interactions in groundwater systems for evaluating recharge, discharge, aquifer storage processes, and sustainable yield, and predicting effects of management measures, thus enabling water managers and decision makers to make informed decisions for sustainable development and management of groundwater resources (Zhou & Li 2011; Rossman & Zlotnik 2013). Over the years, several groundwater flow models such as the United States Geological Survey (USGS) three-dimensional finite difference model (Trescott 1975), the USGS MODFLOW (McDonald & Harbaugh 1988), FEMWATER (Lin *et al.* 1997), HST3D (Kipp 1997), SEEP2D (Jones 1999), SUTRA (Voss & Provost 2002), and FEFLOW (Diersch 2014) have been developed. These simulation models use different numerical discretization schemes, i.e., finite difference (FD), finite element (FE), and finite volume (FV) for solution of the groundwater flow equation. The FD-based MODFLOW uses structured rectangular grids to represent the model domain and maintains mass-balance but fails to simulate complex geological features, such as angled faults and steep hydraulic gradients such as rewetting/drying cells (Kumar 2019). On the other hand, the FE-based commercially available FEFLOW model

uses a triangular mesh to represent the model domain, can incorporate complex geologic features and also simulate wetting/drying of cells, but local mass conservation is not guaranteed (Kumar 2019). The choice of a particular model depends on the complexity of model setup and development, ease and accuracy of representing aquifer systems, availability of data related to aquifer properties and geology of the porous media, the ease with which the model input and output files could be prepared, availability of graphical user interfaces (GUIs), pre- and post-processing modules, project time-frame and cost involved, future use of the model, etc. The MODFLOW model has been widely used worldwide because of its extensive testing, flexible modular structure for integration of additional simulation capabilities, complete coverage of hydrogeological processes, public-domain free availability, and continued institutional support, and is regarded as the industry standard in groundwater modeling (Zhou & Li 2011; Rossman & Zlotnik 2013). There are several Windows-based GUIs, post-processors for MODFLOW such as Processing Modflow (Chiang & Kinzelbach 2001), Visual Modflow (Waterloo Hydrogeologic 2019), Groundwater Vista (Rumbaugh & Rumbaugh 2017), MODPATH (Pollock 2016), etc., which makes the modeling process much easier and saves time in analyzing model results. Other approaches like machine learning and statistical models are also being used to simulate groundwater levels globally (Mohanty *et al.* 2013; Adombi *et al.* 2022), but they work on the statistical relationship between predictors and predictand variables and do not consider associated physical mechanisms. Furthermore, they forecast the long time–series data at a point scale, while MODFLOW has the capability to account for spatial variability in fluxes owing to land use pattern, lithology, physical interaction of surface water bodies, and aquifer systems, in addition to interaction with physical boundaries while simulating the groundwater flow at the regional scale. Thus, this model accounts for all factors and boundary conditions prevailing in the study region, and provides the opportunity to simulate very near to actual conditions. MODFLOW has been successfully applied to study groundwater behavior at different locations of India (Eastern Gangetic Plains of India, Western Uttar Pradesh, western region of Chhattisgarh, Odisha (Mahanadi Delta)) including the study region (Alam & Umar 2013; Sahoo & Jha 2017; Mali *et al.* 2021; Gobinath *et al.* 2022; Kumar *et al.* 2022).

In this study, an attempt has been made to study the combined effect of anticipated changes in rainfall and air temperature on different water budget components (crop evapotranspiration, irrigation requirement, deep drainage, runoff) of a groundwater irrigated rice–wheat dominated cropping region, under two different scenarios of CO_2 concentration, namely, (i) changing CO_2 concentration with time corresponding to different RCPs and (ii) keeping CO_2 concentration constant at a reference (default) level of 369.41 ppm. The AquaCrop and MODFLOW models were used for simulating water budgeting components and their effects on the groundwater of the study region. While the AquaCrop model, capable of accounting for the effect of CO_2 level in estimating daily water balance components, simulates the yield response to water and is mostly used for field-scale irrigation management and water resources planning (Foster *et al.* 2017; Xing *et al.* 2017), the numerical MODFLOW includes complex interactions in groundwater systems (Khadri & Pande 2016; Hughes *et al.* 2022) and is used to simulate spatiotemporal variation in groundwater condition in the study region of northwestern India.

2. MATERIALS AND METHODS

2.1. Brief description of the study area

The study area, covering an area of 2,520 km^2, falls in the semi-arid Indo-Gangetic Plain region of northwest India, between 29°25′05″–29°59′20″ N and 76°27′40″–77°13′08″ E (Figure 1). About 85% of the study area, Karnal district of Haryana province is under the intensive rice–wheat agricultural system. The average annual rainfall and evaporation are 747 mm and 1,610 mm, respectively. Analysis of 30 years (1981–2010) of weather data indicated that almost 75% of the annual rainfall in the region occurs between the first week of July and the first quarter of September, i.e., the monsoon period (Nand *et al.* 2021). The ambient temperature and relative humidity in the study region vary in the range of 3–46 °C and 36%–84%, respectively, during different months of the year.

2.2. Data collection and generation

Weather data on air temperature, rainfall, wind velocity, sunshine hours, and relative humidity for the period 1981–2010 was collected from the meteorological observatory situated at ICAR-Central Soil Salinity Research Institute (CSSRI), Karnal. Since rice–wheat is the dominant cropping system of this region, these two crops were grown in two consecutive crop calendars (2014–2015 and 2015–2016) at the research farm of ICAR-CSSRI, to generate field data (Kumar *et al.* 2022) for parameterization and validation of the AquaCrop model.

For assessing climate change impacts on groundwater levels, the climate change projections of the *Fifth Assessment Report of the Intergovernmental Panel on Climate Change* (IPCC 2013), based on RCPs were used in this study. Bias-corrected and

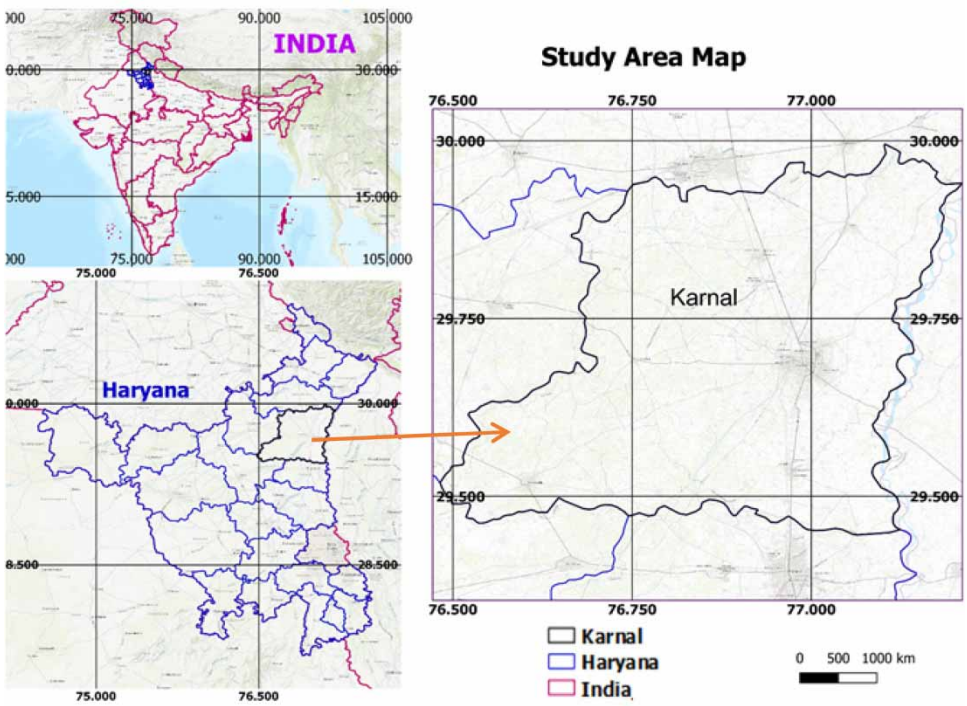

Figure 1 | Location map of the study region.

spatially disaggregated (BCSD) monthly projections of rainfall and temperature for the period 1950–2099 at 0.5° × 0.5° resolution were derived from the World Climate Research Program's (WCRP's) Coupled Model Inter-comparison Project phase 5 (CMIP5) multi-model dataset (https://gdo-dcp.ucllnl.org/downscaled_cmip_projections/dcpInterface.html#Projections:%20Complete%20Archives). The CMIP5 multi-model datasets have been used in several climate change impact studies due to their ability to provide reliable and robust results (Sonali *et al.* 2017; Zhang *et al.* 2019; Abeysingha *et al.* 2020; Doulabian *et al.* 2021; Kumar *et al.* 2022).

2.3. Development of climate change scenarios

Since outputs of different GCMs for some regions vary considerably, there has been growing interest in using multi-model ensembles from multiple GCMs to account for the uncertainty associated with individual GCMs in impact assessment studies. In this study, the hybrid-delta method (Hamlet *et al.* 2010; Islam *et al.* 2012a, 2012b) was used to generate multi-model ensemble climate change scenarios from multiple GCM projections for four different RCPs. The delta change method, the most commonly used method for generating future climate scenarios, does not consider variability or change in time series behavior in the future. On the other hand, the hybrid-delta method considers inter-annual variability for each month (Hamlet *et al.* 2010; Islam *et al.* 2012c; Tohver *et al.* 2014) using different scaling factors to each month of the historic time–series based on where it falls in the probability distribution of monthly values (Dickerson-Lange & Mitchell 2014). In this method, BCSD monthly GCM data (historical as well as future) were first disaggregated into individual calendar months. BCSD monthly GCM data (temperature and precipitation) were derived for historical (1981–2010, base period) and for the future periods of 2010–2039 (early century), 2040–2069 (mid-century), and 2070–2099 (end-century). The cumulative distribution functions (CDFs) were then developed for each month for historical and future time-periods (2020s, 2050s, and 2080s). For creating an ensemble of multiple GCMs/runs, data from multiple GCMs/runs were used for developing historical and future CDFs. Similarly, the CDFs for the observed time series data (1976–2005) were also developed, and the non-exceedance probability for each of the observed data was computed. Quantile mapping (Wood *et al.* 2002) was applied to re-map the observations onto historical and future CDFs for each month to obtain the historical and future GCM projected rainfall and temperature data at non-exceedance probability of the observed data. A step-by-step procedure for generating an ensemble of multiple GCMs using the hybrid-delta method is described in Tohver *et al.* (2014).

The effect of climate variability on water balance components was studied for two scenarios. In Scenario-I, the effect of projected rainfall, maximum and minimum temperature, and CO_2 concentration on evapotranspiration, irrigation requirement, runoff, and deep drainage of the corresponding year was simulated under four RCPs (RCP2.6, RCP4.5, RCP6.0, and RCP8.5). The projected atmospheric CO_2 concentration corresponding to different RCPs is depicted in Figure 2. In Scenario-II, the effect of minimum and maximum temperature and rainfall on the same parameters was evaluated at a constant CO_2 concentration level of 369.41 ppm (corresponding to the concentration of the year 2000) for four RCPs and three future periods.

2.4. Simulation of groundwater level

The modeling approaches and methodology used in this study to simulate interaction between the weather, soil, crop, and groundwater systems under anticipated changes in temperature, rainfall, and CO_2 concentrations are presented in Figure 3. It depicts the interaction between different components, and a step-by-step procedure adopted for simulating the impact of climate change on water budgeting components and groundwater levels in the study region. The widely used AquaCrop model (Steduto *et al.* 2012) was selected to establish relationships among soil, crop, and weather parameters for estimating upward and downward flux from the cropped land, while the Hydrus-1D (Šimůnek *et al.* 2022) model was used for estimating fluxes from the fallow land. The derived fluxes were used as input to a groundwater flow model, MODFLOW (Harbaugh 2005) to simulate future groundwater levels under projected changes in CO_2 concentration, temperature, and rainfall. The MODFLOW model was set up based on lithology, 90×90 m resolution Shuttle Radar Topography Mission (SRTM) digital elevation model (DEM), appropriate boundary conditions, groundwater levels recorded using observation wells, and assigned upward flux and downward flux. MODFLOW was calibrated by adjusting model parameters, i.e., aquifer hydraulic conductivity and storage coefficient to match the observed groundwater levels for a ten-year period (2001–2010). Using the calibrated model parameters, the model was then validated by matching the observed groundwater levels for the 2011–2015 period. The calibrated and validated MODFLOW was later adopted to quantify the impact of climate change parameters on future groundwater behavior in the study area. The full description of the AquaCrop and MODFLOW models and the calibrated parameters and model efficiency is provided in Kumar *et al.* (2022).

The amounts of groundwater withdrawal to meet the water requirements of different sectors including agriculture and replenishment (deep drainage) were treated as upward and downward fluxes, respectively, in the numerical model for simulation of groundwater levels. More than 85% of the study area was covered under the rice–wheat cropping system, while the remaining portion was under plantation, built-up, water sources, and other land uses. The groundwater irrigation (draft) and replenishment (deep drainage) from the rice–wheat cropping system were simulated using the AquaCrop model. The draft and replenishment components for other land uses were estimated using the standard procedures and methodology (GEC

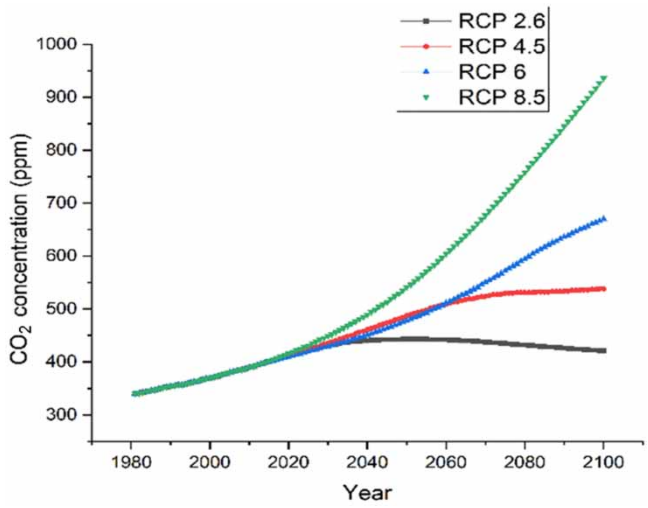

Figure 2 | Projected atmospheric CO_2 concentration under different RCPs.

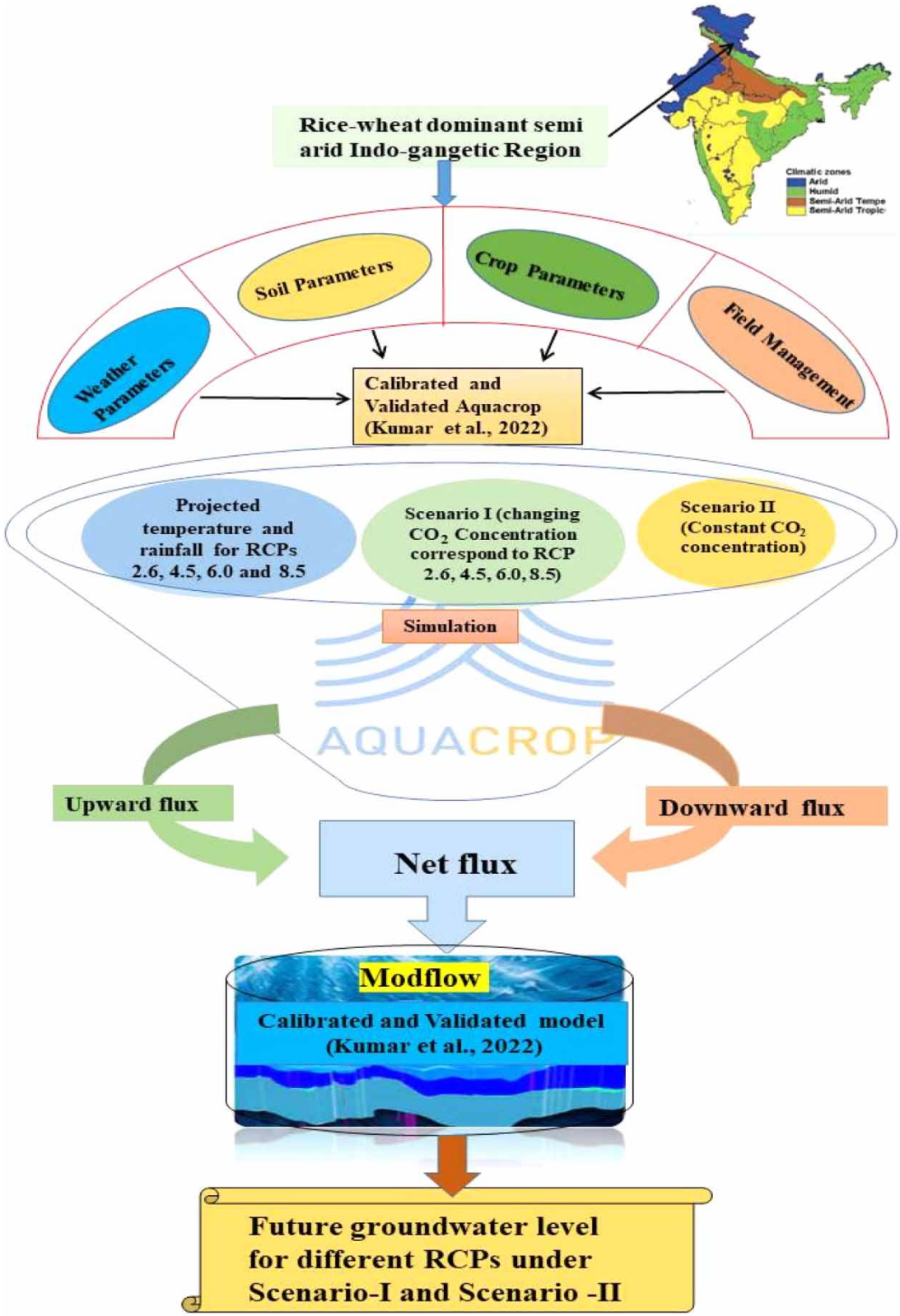

Figure 3 | Graphical representation of the methodological process adopted in the present study.

2009; Narjary *et al.* 2021; Kumar *et al.* 2022). The general methodology used for calculating upward and downward flow components is briefly described below.

2.5. Upward fluxes

The upward flux from the experimental rice–wheat fields was estimated using the AquaCrop model considering weather, soil, and crop data and the water application criterion (Raes *et al.* 2022). Similarly, the draft for the domestic sector was calculated by considering human water consumption of 200 litres day^{-1} per person (Shaban & Sharma 2007) and the population of the area derived from the census data (www.census2011.co.in/district.php). The upward flux from the plantation area was estimated considering the water consumption of 1,500 mm year^{-1} for the *Eucalyptus* plantation (Minhas *et al.* 2015), which was the major tree planted in the study area (Kumar *et al.* 2022). It was assumed that groundwater pumping will be zero in the remaining parts of the study area because either land was barren or under water bodies.

2.6. Downward fluxes

A downward flux in the form of deep drainage to replenish the groundwater was similarly estimated for rice–wheat cropping systems and other land uses. Deep drainage from the rice–wheat fields was calculated through the AquaCrop model (Xu *et al.* 2019) using the following equation:

$$D_d = (I_r + (R_a) - ET_c - R_o \pm \Delta S \quad (1)$$

where D_d is deep drainage in mm, I_r is the irrigation application depth (mm), R_a is the precipitation (mm), ET_c is the crop evapotranspiration (mm), ΔS is the change in moisture in the root zone (mm), and R_o is the runoff from the field (mm) in a specific period. It was considered that D_d, i.e., moisture leaving the crop root zone, will eventually meet the aquifer, sooner or later, and contribute to the replenishment of groundwater. The contribution to groundwater from the fallow land was calculated using the Hydrus-1D model (Narjary *et al.* 2021). The deep drainage from the built-up area was estimated as the amount of rainfall exceeding surface runoff assuming nil evapotranspiration losses (Kumar *et al.* 2022). Evapotranspiration (ET) from the built-up area was neglected because it is considerably less than other land uses due to contrasts in the hydrological properties of building materials and vegetation-covered soils (Chandler 1976). Contribution from canal seepage was estimated using the methodology described in the groundwater resource estimation committee report (GEC 2017).

3. RESULTS

3.1. Change in temperature and rainfall during rice and wheat crop period

The projected change in temperature and rainfall during the rice-growing season for the future periods was analyzed in relation to the mean value of the base period (1981–2010). For the base period, the average maximum and minimum temperature and rainfall during the rice-growing season (July–October) were 32.9 °C, 23.3 °C, and 529.5 mm, respectively. The average temperature during the rice-growing season (June–November) is projected to increase in the range of 1.0–1.3 °C, 1.6–2.7 °C, and 1.7–4.6 °C over the base period during the early, mid-, and end-century periods, respectively, under different RCPs (Figure 4(a)). The maximum temperature is projected to rise in the range of 0.8–1 °C, 1.4–2.3 °C, and 1.6–4.1 °C, while the minimum temperature is projected to rise in the range of 1.3–1.5 °C, 1.2–3.1 °C, and 1.9–5.1 °C over the base period values during the early, mid-, and end-century periods, respectively, under different RCPs (Figure 4(a)). Among different RCPs, the RCP8.5 resulted in maximum increases of 1.0, 2.3, and 4.1 °C in maximum temperature, and 1.5, 3.1, and 5.1 °C in minimum temperature during early, mid-, and end-century, respectively. Interestingly, the rise in minimum temperature is greater than that of maximum temperature (Figure 4(a)). Rainfall during the rice-growing season is also projected to increase under all four RCPs during three future periods in the range of 6.5% (RCP8.5)–8.3% (RCP4.5), 8.9% (RCP6.0)–13.1% (RCP8.5), and 7.6% (RCP2.6)–21.2% (RCP8.5) during the early, mid-, and end-century, respectively (Supplementary Table S1). Interestingly, an increase in rainfall is projected to be lower under RCP2.6 during the end-century period than the mid- and early century periods, while a gradual increase in rainfall is projected during the early century period (6.5%), the mid-century period (13.1%), and the end-century period (21.2%) under RCP8.5.

In relation to crop seasons, a comparatively higher increase in maximum and minimum temperatures was projected during the wheat-growing season (November–April) under all RCPs. The mean temperature, maximum temperature, and minimum temperature are projected to increase in the range of 1.3–1.6 °C, 1.2–1.5 °C, and 1.4–1.7 °C, respectively, during the early

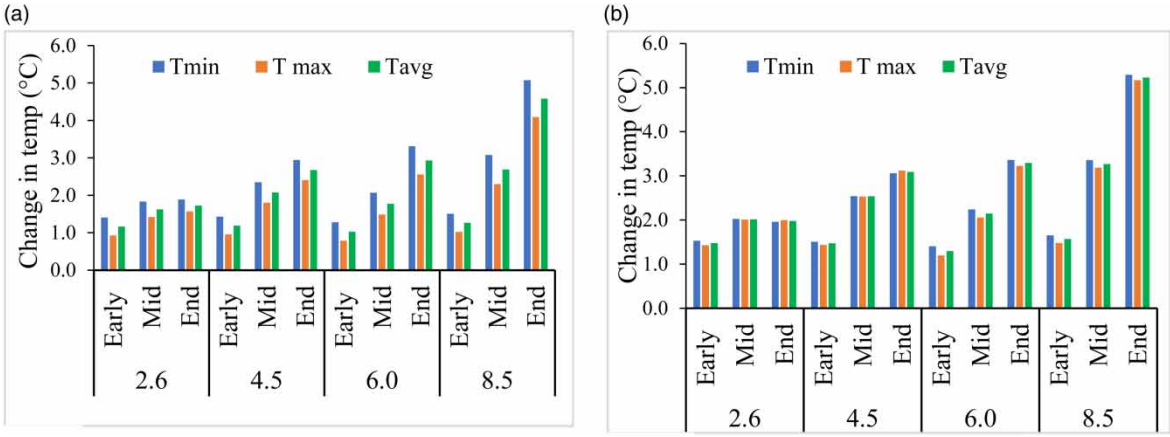

Figure 4 | Projected change in min (T_{min}), max (T_{max}), and average (T_{avg}) temperature during (a) rice- and (b) wheat-growing seasons in the early (2011–2039), mid- (2040–2069), and end-century (2070–2099) periods with reference to the base period (1981–2010).

century under different RCPs (Figure 4(b)). Similarly, the mean, maximum and minimum temperatures are projected to increase in the range of 2.0–5.2 °C, 2.0–5.2 °C, and 2.0–5.3 °C, respectively, during the end-century under different RCPs (Figure 4(b)). Similar to rice, the wheat-growing season also recorded a greater increase in minimum temperature than that of maximum temperature during all the future periods. During the wheat-growing season too, there is a marginal increase (≤10%) in rainfall under all RCPs. The increase in rainfall varied in the range of 5.3% (RCP2.6)–8.4% (RCP6.0), 3.3% (RCP8.5)–5.8% (RCP6.0), and 3.1% (RCP8.5)–8.4% (RCP2.6), during the early, mid-, and end-century periods, respectively. Though there is an increase in rainfall during the wheat-growing season under RCP8.5, this increase in rainfall gradually decreases from the early century (6.9%) to mid-century (3.9%) and to the end-century periods (3.1%) (Supplementary Table S2).

3.2. Water budgeting components

The field water budgeting components (crop evapotranspiration, irrigation water requirement, deep drainage, and runoff) under different climate change scenarios were simulated and the changes were analyzed with reference to the mean value of the particular component for the base period.

3.2.1. Crop evapotranspiration

The mean evapotranspiration of the rice crop (ET_{cr}) was estimated as 475.10 mm for the base period (1981–2010). ET_{cr} was found to be higher in Scenario-II (constant CO_2 concentration) as compared with Scenario-I (increasing CO_2 concentration) under all RCPs during the simulation periods (Figures 5(a) and 6(a)). For instance, ET_{cr} in Scenario-II is projected to increase in the range of 2.3%–3.1%, 0.7%–4.2%, and 3.6%–5.5% during the early, mid-, and end-century periods, while it is projected to decrease during the mid- and end-century periods in Scenario-I (Supplementary Table S2). The change in ET_{cr} varied in the range of 1.5%–1.8%, −2.8%–2.8%, and −4.4%–4.2% during the early, mid-, and end-century periods, respectively, under different RCPs under Scenario-I.

The average (1981–2010) wheat crop evapotranspiration (ET_{cw}) was estimated as 368.8 mm. An increase in ET_{cw} over the base period is projected for both scenarios under all the RCPs and future periods, however, with ET_{cw} being higher in Scenario-II than in Scenario-I. In Scenario-I, the increase in ET_{cw} varied in the range of 43.8%–48.3% under different RCPs in the three future periods (Figures 5(b) and 6(b)) (Supplementary Table S2), whereas in Scenario-II, the increase in ET_{cw} varied in the range of 45.4%–61.4%. Furthermore, the increase in ET_{cw} is projected to be higher during the end-century period as compared with the mid- and early-century periods. Of all RCPs, the maximum increase of 48.3% and 61.4% in ET_{cw} from the reference level (368.8 mm) is projected under RCP4.5 (Scenario-I) and RCP8.5 (Scenario-II), respectively, during the end-century.

3.2.2. Irrigation water requirement (IR)

The average rice irrigation requirement (IR_r) of the base period (1981–2010) was estimated as 1,146.2 mm. A marginal (<10%) decrease in IR_r is projected during future periods under all RCPs for both scenarios, except for an imperceptible increase of 0.3% under RCP2.6 and Scenario-II during the end-century period (Figures 5(a) and 6(a)). IR_r under Scenario-I is projected to decrease in the range of 0.7%–6.0% considering all future periods and RCPs, the corresponding range for

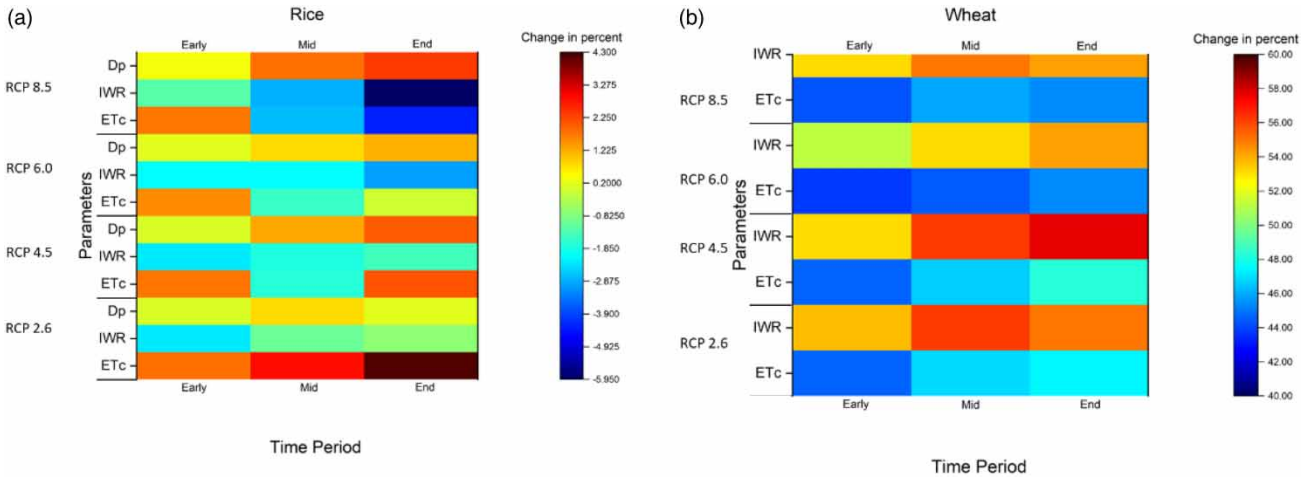

Figure 5 | Change in (a) rice and (b) wheat water budgeting parameters under Scenario-I (elevated CO_2, temperature, and rainfall) during the early (2011–2039), mid- (2040–2069), and end-century (2070–2099) periods with reference to the base period (1981–2010).

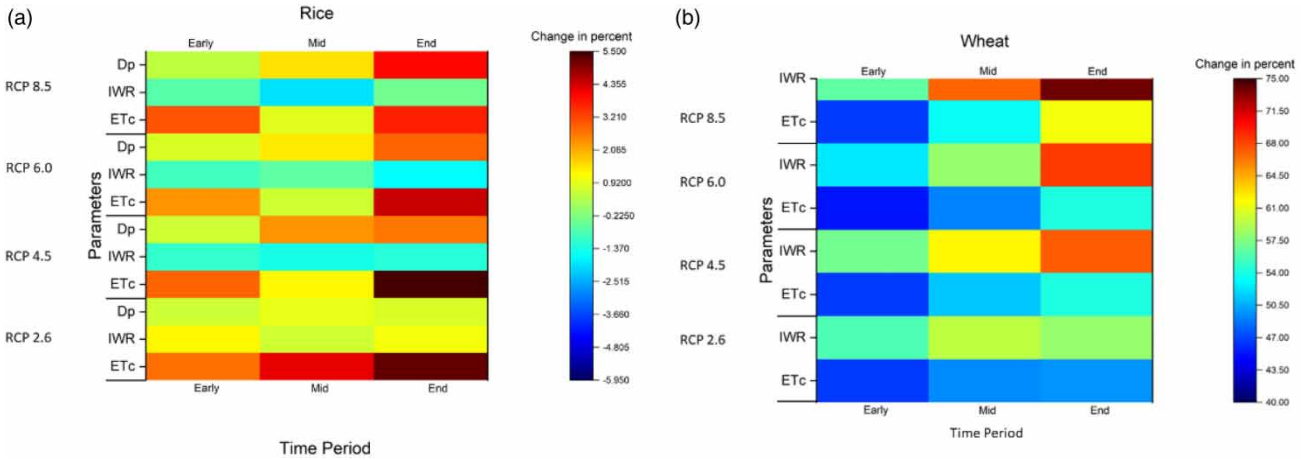

Figure 6 | Change in (a) rice and (b) wheat water budgeting components under Scenario-II (increasing temperature, rainfall, and constant CO_2 concentration) during the early (2011–2039), mid- (2040–2069), and end-century (2070–2099) periods with reference to the base period (1981–2010).

Scenario-II being 0.3%–1.6% (Figures 5(a) and 6(a)). Hence, IR_r is projected to decrease 2.3%–6.3% more in Scenario-I than in Scenario-II. The average wheat irrigation requirement (IR_w) was estimated as 308.3 mm for the base period. Similar to the wheat crop evapotranspiration, there is an increase in IR_w during the future periods, and it has a similar pattern as that of crop evapotranspiration. The wheat irrigation requirement during the future periods is projected to increase in the range of 51.1%–57.7% and 52.5%–73.8% under Scenario-I and Scenario-II, respectively, as compared with the base period under different RCPs and future periods (Figures 5(b) and 6(b)) (Supplementary Table S2). Hence, an increase in irrigation requirement is projected to be 1.4%–16.1% higher in Scenario-II than in Scenario-I. It was also found that the change in IR_w is maximum under RCP2.6 and minimum under RCP6.0 in Scenario-I. However, in the case of Scenario-II, the highest and the lowest change in IR_w is projected under RCP8.5 and RCP2.6, respectively.

3.2.3. Deep drainage (D_d)

Since deep drainage (D_d) was negligible in the wheat crop, D_d from the rice field only is discussed here. In the case of the rice field, the increase in D_d is projected to be less than 5% under all RCPs and future periods. The increase in D_d was found to be higher (0.4%–4.0%) in Scenario-II than in Scenario-I (0%–2.4%). Simulation results also indicated that D_d would be the highest under RCP8.5 and the lowest under RCP2.6 for both the scenarios of CO_2 concentration (Scenario-I and II).

3.2.4. Runoff

As there was no runoff during the wheat season, runoff from the rice crop field is discussed here. Simulation results showed an increase in runoff under different RCPs in the three future periods with slightly higher increase when CO_2 concentration was kept constant (Scenario-II) than in the case of increasing CO_2 concentrations (Scenario-I). Runoff is projected to increase by 27.9%, 56.7%, and 62.2% vis-à-vis for the base period (14.7 mm) in Scenario-I and by 30.6%, 58.4%, and 64.4% in Scenario-II under RCP2.6 during the early, mid-, and end-century periods, respectively (Figures 5(a) and 6(a)) (Supplementary Table S1). The maximum and minimum increase in runoff is projected under RCP8.5 and RCP2.6, respectively, in both the scenarios (Scenario-I and Scenario-II) for the simulation periods. Irrespective of climate scenarios, the increase in runoff was the maximum during the end-century and the minimum during the early century period.

3.3. Groundwater level (GWL)

Fluctuations in groundwater level (GWL) under both the scenarios were compared with the GWL of 18.85 m of the reference year (2015). The groundwater levels are projected to decline to 28.3, 42.4, and 55.4 m at the end of the early, mid-, and end-century periods, respectively, under RCP2.6 in Scenario-I (increasing CO_2 concentration during the future periods) from the reference GWL. However, for Scenario-II (CO_2 concentration was kept constant at 369.41 ppm), the GWLs are projected to decline to 29.1, 44.9, and 59.1 m by the end of the early, mid-, and end-century periods, respectively, from the reference level, under RCP2.6 (Figure 7). Under RCP8.5, the GWL is projected to decline by 9.2, 20.5, and 24.4 m at the end of the early, mid-, and end-century periods, respectively, in Scenario-I from the reference GWL of 18.85 m, whereas it is projected to decline by 10.7, 26.9, and 40.5 m at the end of the early, mid-, and end-century periods under Scenario-II. Thus, under RCP8.5, a lesser decline of 1.5, 6.4, and 16.1 m in GWL at the end of early, mid-, and end-century, respectively, is projected under Scenario-I than Scenario-II. A similar trend is projected for RCP4.5, RCP6.0, and RCP8.5 but with varying magnitude. Therefore, a lesser GWL decline is projected in Scenario-I than Scenario-II. By the end of the simulation period (2099), an additional decline in GWL of 3.7, 8.2, 9.0, and 16.1 m, is projected in Scenario-II as compared with Scenario-I under RCP2.6 (CO_2 level: 419–441 ppm), RCP4.5 (CO_2 level: 422–532 ppm), RCP6.0 (CO_2 level: 418–611 ppm), and RCP8.5 (CO_2 level: 432–800 ppm), respectively.

4. DISCUSSION

4.1. Changes in future temperature and rainfall

Our results indicated an increase in maximum and minimum temperature during future periods, and this increase is projected to be higher during the wheat-growing season (November–April) than in the rice-growing season (June–October). These results are in confirmation with the finding of a study conducted in central India where 1–5 °C increase in maximum and minimum temperature was reported for the winter season coinciding with the wheat-growing period as compared with 1–3 °C increase during the summer season (Kundu *et al.* 2017). Our results are also in close proximity to the reported projected rise in mean temperature of 3.11 and 5.46 °C under RCP4.5 and RCP6.0, respectively, for the end-century period (Dar *et al.* 2019). However, the projected rise in mean temperature (2.5–4.4 °C) reported by Bal *et al.* (2016) for India was less than the projection made in the present study. Sanjay *et al.* (2020) also reported a mean temperature rise of 4 °C under RCP8.5 at the end-century period for most parts of India and still higher (>5 °C) for semi-arid northwest and north India. It is therefore clear that though the magnitude of changes in projected temperature can vary from place to place depending upon the areal extent considered, the rise in temperature is imminent in the coming future. Our study also projects an increase in rainfall during future periods, up to 21% during the rice-growing monsoon season and <10% during the wheat-growing winter season. Bal *et al.* (2016) also projected an average increase in rainfall in the range of 15%–24% for all of India. Dar *et al.* (2019) also projected a similar, though slightly higher increase in rainfall, while Kulkarni *et al.* (2020) reported a lower (10%) increase in mean annual precipitation under RCP4.5 for the mid-century period, and more than 20% increase for the end-century period over northwest India. The present study and results of the other studies conducted elsewhere revealed an increase in rainfall, though with varying magnitude, during future periods due to climate change effects. The present study also revealed that an increase in temperature during the rice as well as the wheat-growing season is likely to increase evapotranspiration, and thereby crop water demand and irrigation requirement. But, an increase in rainfall during the rice-growing season may offset the effect of increased temperature on the rice irrigation requirement. However, the wheat irrigation requirement is projected to increase in future owing to a rise in crop water demand due to rising temperature because only a slight increase (<10%) in rainfall is projected.

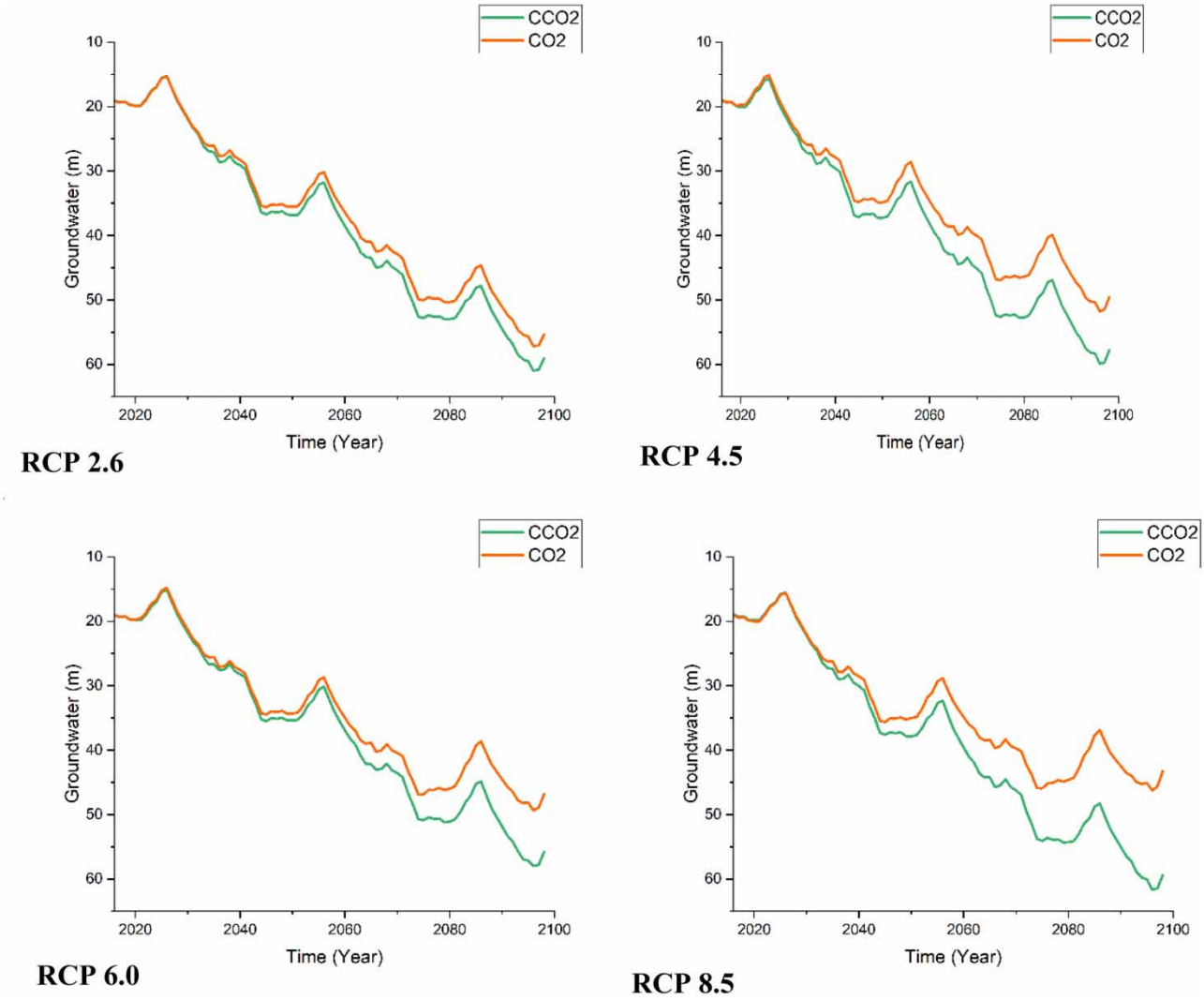

Figure 7 | Change in groundwater level under Scenario-I (elevated CO_2 concentration (CO_2), temperature, and rainfall) and Scenario-II (constant CO_2 concentration (CCO_2), temperature, and rainfall).

4.2. Water budgeting components

4.2.1. Crop evapotranspiration

Simulation results showed lower crop evapotranspiration of rice (ET_{cr}) in Scenario-I as compared with that of Scenario-II during the future periods. The lower increase in ET_{cr} during the future periods may be attributed to the steady increase in CO_2 concentration under Scenario-I as compared with Scenario-II, where CO_2 concentration remained constant (i.e., 369.4 ppm) during the future periods. The increased CO_2 concentration results in reduced stomatal opening and thereby reduced ET (Yang & Lei 2022). Some previous studies also showed that rising CO_2 concentration decreases the stomatal conductance, which causes lower transpiration and thus crop evapotranspiration (Bernacchi *et al.* 2007; Lenka *et al.* 2020; Liao *et al.* 2021). Allen *et al.* (2003) also reported that an increase in CO_2 concentrations from 350 to 700 ppm reduced soybean evapotranspiration. Ficklin *et al.* (2010) also reported a decrease in daily alfalfa ET (-0.3 and -0.9 mm day^{-1}) under increasing temperature ($+1.1$ and 6.4 °C) and CO_2 (550 and 970 ppm) concentration. This confirms that rising CO_2 concentration impacts crop evapotranspiration, though the magnitude is variable for different crops. Furthermore, in Scenario-II (constant CO_2 concentration), rice evapotranspiration (ET_{cr}) is projected to increase during the future periods under all RCPs with different magnitudes. Our results project an increase of 1–5 °C in air temperature, which might have increased the drying

capacity of the atmosphere, thus leading to more evapotranspiration. Abeysingha *et al.* (2016) also reported a 3%–9.6% increase in rice evapotranspiration (ET_{cr}) at the end of the 21st century under rising temperature with a constant CO_2 scenario that concurs well with the present study for Scenario-II. Our study also revealed that ET_{cr} would increase steadily during the future periods in Scenario-I under RCP2.6 in which the CO_2 level is projected to increase until the end of the early century and have a slightly decreasing trend thereafter. This premise is that the increasing temperature might be the dominant factor for increase in ET_{cr} under RCP2.6. In contrast, ET_{cr} is projected to decrease gradually under RCP8.5 during the mid- and end-century periods. A substantial increase in projected CO_2 concentration under RCP8.5 during the mid- and end-century periods might have negated the effect of increasing temperature on ET_{cr} (Ficklin *et al.* 2010). Allen *et al.* (2003) also reported that a doubling of CO_2 concentration results in a reduction in ET of rice by 9%. Priya *et al.* (2014) also reported that the effect of a 2.5 °C rise in temperature in Varanasi, India, was offset by an increase in CO_2 levels up to 660 ppm.

Results of our study also projected increasing wheat crop evapotranspiration (ET_{cw}) during the future periods in both scenarios (I and II) under all RCPs. However, an increase in ET_{cw} will be slightly lower in Scenario-I than Scenario-II, probably due to the dominance of increasing CO_2 concentration over lower temperatures as wheat in this area is grown during the winter season where most of the time, the maximum temperature varies between 5 and 30 °C. Results of this study are in line with the finding of Allen *et al.* (2003) who reported that the increase in CO_2 concentration from 350 to 700 ppm reduced the crop evapotranspiration in the temperature range of 18–28 °C, while there was little effect in the temperature range of 30–40 °C. Shimono *et al.* (2013) also observed reduction in evapotranspiration because of elevated CO_2 and affected by higher temperatures. This suggests that elevated CO_2 effects might be moderated by higher ambient temperature. A considerable increase in ET_{cw} over the simulation period was simulated in Scenario-II also, which indicates an effect of rising temperature during a wheat-growing period (Nand *et al.* 2021). The finding of the present study confirms the trend of previous findings (Chattaraj *et al.* 2014; Abeysingha *et al.* 2016; Dar *et al.* 2017; Qu *et al.* 2019), which revealed an increase of 7.8% to 16.3% in ET_{cw} at the end of the 21st century under different rising temperature scenarios. Hence, the overall results of the present study clearly indicate that an increase or decrease in future ET is driven both by rising temperature as well as variable CO_2 concentration; the dominant factor being dependent on the level of increase in temperature and CO_2. Savabi & Stockle (2001) reported that ET_c of corn decreased when the mean temperature increased by 1.2 °C and CO_2 increased to 480 ppm. However, when the average temperature increased beyond 1.2 °C and CO_2 exceeded 480 ppm, ET_c rose marginally. In a soybean crop, increase in CO_2 concentration from 330 to 350 ppm and increase in daily average temperature by 2.8 °C resulted in an increase in ET_c by 4%, while in the case of constant temperature and rising CO_2 scenario, ET_c reduced considerably.

4.2.2. Irrigation water requirement

Our study showed a decrease in irrigation requirement of the rice crop (IR_r) during future time periods in both the scenarios (I and II) under all RCPs due to an increase in rainfall. Furthermore, the projected steady increase in CO_2 concentration under Scenario-I also resulted in reduced evapotranspiration and rice irrigation requirement compared with constant CO_2 concentration (Scenario-II). Hence, the effect of rising temperature on IR_r is probably moderated by the increasing CO_2 concentration effects on crop evapotranspiration (Allen *et al.* 2003; Priya *et al.* 2014; Lenka *et al.* 2021; Yang & Lei 2022). The highest decrease in IR_r is projected for the end-century period under RCP8.5 in Scenario-I as the lowest ET_{cr} and the highest rainfall were projected during the end-century period under RCP8.5. However, in Scenario-II, increasing rainfall has a singular impact on IR_r under constant CO_2 concentration resulting in a lower decrease in IR_r than in Scenario-I. Our results confirm the observations of Abeysingha *et al.* (2016), who projected a <5% decrease in irrigation requirement of rice in north India due to an increase in rainfall at the end of the year 2099 and also projected a decline in IR_r for future periods. Dar *et al.* (2017) also projected a decline in rice irrigation in future under changing climate.

Our results showed an increase in irrigation water requirement of the wheat crop (IR_w) also during the future periods under all RCPs in both the scenarios (I and II). This may be attributed to a substantial increase in ET_{cw} with rising temperature and negligible (<10%) increase in rainfall during the wheat-growing period. Similar to ET_{cw}, simulated IR_w is slightly higher in Scenario-II than in Scenario-I. The present study also projects a significant reduction in IR_w in Scenario-I under RCP8.5 due to a lesser ET_{cw} because of a considerable increase of CO_2 concentration. Our estimates of increase in IR_w during the future time-periods are also in agreement with the findings of other studies of variable changes in wheat irrigation requirements under projected variability (rise or fall) in rainfall amount (Abeysingha *et al.* 2016; Xiao *et al.* 2020).

4.2.3. Deep drainage

Our study projected negligible deep drainage (D_d) from the wheat field during the future periods. This might be due to the fact that a limited rainfall amount is expected during the winter season that could be effectively utilized by the crop or stored within the root zone. In contrast, an increase (though less than 5%) in D_d is projected from the rice field during future periods that could be attributed to projected higher rainfall and irrigation during the rice-growing period. The irrigation criterion to apply water at field capacity (Kumar *et al.* 2019) led to higher irrigation and consequent enhanced D_d from the rice fields.

The study further projected higher D_d in Scenario-II than in Scenario-I during the future periods. The lower irrigation associated with lower ET_{cr} under elevated CO_2 in Scenario-I resulted in lower D_d. In Mediterranean climatic conditions, van Ittersum *et al.* (2003) also reported a decrease in deep drainage from a wheat field under increasing temperature and elevated CO_2 concentration. Ficklin *et al.* (2010) also reported a decrease in deep drainage under elevated CO_2 and temperature, and projected a decline in cumulative groundwater recharge for alfalfa, almonds, and tomato crops.

4.2.4. Runoff

Our simulation results showed an increase in runoff from rice fields during the future periods under all RCPs in both the scenarios of CO_2 concentrations (Scenario-I and II) due to the projected increase in rainfall. However, a negligible difference in simulated runoff under Scenario-I and Scenario-II indicates that rising temperature and CO_2 concentration may not have a substantial effect on runoff from the irrigated cropped land, and increasing rainfall might be the dominant factor affecting the runoff during the rice-growing monsoon season. Furthermore, the present study area is an irrigated land having almost flat topography where fields have ~10 cm effective bund (embankment) height. The flat topography and on-farm rainfall storage, facilitated by field bunds, might be the reason for little effect of climate change on runoff during the simulation period. This is in contrast to a reported increase in runoff at the watershed level under elevated CO_2 and higher temperature and resulting reduction in crop evapotranspiration (Leipprand & Gerten 2006; Niu *et al.* 2013; Butcher *et al.* 2014). Islam *et al.* (2012c) also reported that changes in temperature had a relatively lesser effect on the magnitude of annual and seasonal stream flow as compared with rainfall changes in the Brahmani River basin. Our results also project the highest and lowest runoff under RCP8.5 and RCP2.6, respectively. Under RCP8.5, an increase in rainfall of 6.5%, 13.1%, and 21.2% resulted in higher runoff than the runoff resulting from 7.8%, 9.0%, and 7.6% rises in rainfall under RCP2.6 during early, mid-, and end-century, respectively. Working on Dez basin in Iran, Ehteram *et al.* (2018) reported that reduction in precipitation amounts in the future period (2011–2030) is the major reason for decreased runoff volume.

4.3. Groundwater levels

Our study showed a lower GWL decline under Scenario-I (increasing CO_2 concentration) than Scenario-II (constant CO_2 concentration) during the future periods. Hence, it is clear that the GWL decline is associated with CO_2 concentration as it influences crop evapotranspiration and consequently irrigation demand. Our study projects almost identical changes in GWL for the early century period in both the scenarios of CO_2 concentration (Scenario-I and II) due to negligible variation in irrigation demand under all RCPs. However, a remarkably lower GWL decline during the mid- and end-century periods is projected under elevated CO_2 (Scenario-I) than constant CO_2 (Scenario-II). The variation in GWL decline during the mid- and end-century periods may be due to the fact that in Scenario-I, elevated CO_2 might have offset the effects of rising temperature on crop ET, resulting in reduced groundwater withdrawal, which might not have occurred in Scenario-II due to the constant CO_2 concentration (Ficklin *et al.* 2010). This could be the reason for the highest projected increase in CO_2 concentration under RCP8.5 resulting in the lowest decline in GWL among all RCPs from the reference level.

5. SUMMARY AND CONCLUSIONS

In agricultural dominant groundwater irrigated regions, crop water requirement has profound impact on groundwater resources. It is expected that any change in temperature, precipitation, and elevated CO_2 concentration owing to climate change is likely to influence field water budgeting components (crop ET, irrigation, runoff, and deep percolation) and groundwater resources. Therefore, it is necessary to study the integrated effect of increasing CO_2 concentrations along with the change in rainfall and temperature regimes on field water budgeting components and consequently on the groundwater resources during future periods. The present study indicates that irrespective of RCPs, the rice irrigation requirement would decrease slightly (0.7%–6%) during future periods under both increasing (Scenario-I) and constant (Scenario-II) CO_2 concentration scenarios. In contrast, the wheat irrigation requirement is projected to increase significantly (53%–74%)

under Scenario-I and Scenario-II. Furthermore, under RCP8.5, GWL is projected to decline by 9.2, 20.5, and 24.4 m from the reference level (18.85 m) at the end of the early, mid-, and end-century periods, respectively, in Scenario-I, whereas under Scenario-II, it is projected to decline by 10.7, 26.9, and 40.5 m from the reference GWL at the end of the early, mid-, and end-century periods, respectively. This suggests that the effect of rising temperature on irrigation requirements and groundwater decline may be moderated to some extent by elevated CO_2 concentration. Overall, the study emphasizes that CO_2 concentration, temperature, and rainfall must be considered in an integrated way while simulating the impact of climate change on groundwater and for devising sustainable mitigation and adaptation strategies in irrigated agricultural systems.

Though this study provides valuable information on the integrated effects of CO_2 concentration, temperature, and rainfall changes due to climate change on water budgeting components and groundwater, there may be uncertainty in the estimated components due to the model structure/model algorithms, and model parameters. Multi-crop models, rather than a single crop model like AquaCrop, may provide more realistic results in simulating the effect of increasing CO_2 concentrations, temperature, and rainfall change on water balance components (including groundwater) of irrigated agricultural areas. The median or average of the simulated water budgeting components of multi-crop models may be used in future studies for simulating the unified impact of climate change parameters on groundwater resources in an irrigated ecosystem and for formulating sustainable strategies for its optimal management. Further, in the present study, the estimated fluxes from different models/sources were loosely coupled with Visual MODFLOW Flex for groundwater simulation. The MODFLOW model used in this study considers constant fluid density, and does not simulate water flow in dry cells (unsaturated zone) and stream flow–aquifer interaction, although the model limitation of considering constant fluid density does not have much relevance in this study as fluid quality in the aquifer was very similar in the entire study area. However, better handling of water flow in dry cells can improve accuracy and reliability of the model results (Hunt & Feinstein 2012). A recent version of USGS Modflow (Modflow 6) simulates the water flow in dry cells as well as stream flow–aquifer interaction (Langevin *et al.* 2017). Thus, its use in future studies to represent aquifer systems more precisely may improve groundwater simulation further, and aid in developing robust groundwater management strategies for groundwater irrigated rice–wheat dominated cropping regions.

ACKNOWLEDGEMENTS

The authors acknowledge the Director, ICAR-CSSRI, Karnal (Research article/41/2022) for extending logistics support during the execution of this study.

ETHICAL APPROVAL

This article does not report on or involve the use of any animal or human data or tissue.

CONSENT TO PARTICIPATE

This article does not contain data from any individual person.

CONSENT TO PUBLISH

All the authors have given their consent to publish the manuscript.

AUTHORS CONTRIBUTIONS

S.K.: conceptualized the methodology, supervision of work, and manuscript editing; V.N.: calibration and validation of MODFLOW and AquaCrop models; B.N.: data analysis and writing manuscript; P.K.H.: modeling and GIS work; A.I.: GCM projections and climate change projection, manuscript editing; R.K.Y.: field study; S.K.K.: refinement of methodology and editing results and discussion.

FUNDING

This research was funded by the Indian Council of Agricultural Research (ICAR) through the National Innovations in Climate Resilient Agriculture (NICRA) program.

DATA AVAILABILITY STATEMENT

Data that support the findings of this study are available from the corresponding author upon reasonable request.

CONFLICT OF INTEREST

The authors declare there is no conflict.

REFERENCES

Abeysingha, N. S., Singh, M., Islam, A. & Sehgal, V. K. 2016 Climate change impacts on irrigated rice and wheat production in Gomti River basin of India: a case study. *Springer Plus* **5**, 1250. https://doi.org/10.1186/s40064-016-2905-y.

Abeysingha, N. S., Islam, A. & Singh, M. 2020 Assessment of climate change impact on flow regimes over the Gomti River basin under IPCC AR5 climate change scenarios. *Journal of Water and Climate Change* **11** (1), 303–326. https://doi.org/10.2166/wcc.2018.039.

Adombi, A. V. D. P., Chesnaux, R. & Boucher, M.-A. 2022 Comparing numerical modelling, traditional machine learning and theory-guided machine learning in inverse modeling of groundwater dynamics: a first study case application. *Journal of Hydrology* **615**, 128600. https://doi.org/10.1016/j.jhydrol.2022.128600.

Alam, F. & Umar, R. 2013 Groundwater flow modelling of Hindon-Yamuna interfluve region, Western Uttar Pradesh. *Journal of the Geologic Society of India* **82**, 80–90. https://doi.org/10.1007/s12594-013-0113-8.

Allen, L. H., Pan, D., Boote, K. J., Pickering, N. B. & Jones, J. W. 2003 Carbon dioxide and temperature effects on evapotranspiration and water use efficiency of soybean. *Agronomy Journal* **95** (4), 1071–1081.

Andaryani, S., Nourani, V., Pradhan, B., Ansarudi, T. J., Ershadfath, F. & Haghighi, A. T. 2022 Spatiotemporal evaluation of future groundwater recharge in arid and semi-arid regions under climate change scenarios. *Hydrological Sciences Journal* **67** (6), 979–995. https://doi.org/10.1080/02626667.2022.2050732.

Bal, P. K., Ramachandran, A., Palanivelu, K., Thirumurugan, P., Geetha, R. & Bhaskaran, B. 2016 Climate change projections over India by a downscaling approach using PRECIS. *Asia-Pacific Journal of Atmospheric Sciences* **52** (4), 353–369.

Bernacchi, C. J., Kimball, B. A., Quarles, D. R., Long, S. P. & Ort, D. R. 2007 Decreases in stomatal conductance of soybean under open-air elevation of [CO_2] are closely coupled with decreases in ecosystem evapotranspiration. *Plant Physiology* **143**, 134–144.

Bhargava, S. & Mitra, S. 2021 Elevated atmospheric CO_2 and the future of crop plants. *Plant Breeding* **140**, 1–11.

Butcher, J. B., Johnson, T. E., Nover, D. & Sarkar, S. 2014 Incorporating the effects of increased atmospheric CO_2 in watershed model projections of climate change impacts. *Journal of Hydrology* **513**, 322–334.

Chandler, T. J. 1976 *Urban Climatology and Its Relevance to Urban Design*. WMO Technical Note 149, World Meteorological Organization, Geneva, Switzerland.

Chattaraj, S., Chakraborty, D., Sehgal, V. K., Paul, R. K., Singh, S. D., Daripa, A. & Pathak, H. 2014 Predicting the impact of climate change on water requirement of wheat in the semi-arid Indo-Gangetic Plains of India. *Agriculture Ecosystems & Environment* **197**, 174–183. https://doi.org/10.1016/j.agee.2014.07.023.

Chiang, W. H. & Kinzelbach, W. 2001 *3D-Groundwater Modeling with PMWIN: A Simulation System for Modeling Groundwater Flow and Pollution*. Springer-Verlag, New York, USA.

Dar, M., Aggarwal, R. & Kaur, S. 2017 Effect of climate change scenarios on yield and water balance components in rice–wheat cropping system in Central Punjab, India. *Journal of Agrometeorology* **19**, 226–229.

Dar, M. U. D., Aggarwal, R. & Kaur, S. 2019 Climate predictions for Ludhiana District of Indian Punjab under RCP4.5 and RCP8.5. *International Journal of Environment and Climate Change* **9**, 128–141.

Dickerson-Lange, S. E. & Mitchell, R. 2014 Modeling the effects of climate change projections on streamflow in the Nooksack River basin, Northwest Washington. *Hydrological Processes* **28**, 5236–5250.

Diersch, H.-J. G. 2014 *FEFLOW: Finite Element Modeling of Flow, Mass and Heat Transport in Porous and Fractured Media*. Springer, Berlin, Germany. https://doi.org/10.1007/978-3-642-38739-5.

Doulabian, S., Golian, S., Toosi, A. S. & Murphy, C. 2021 Evaluating the effects of climate change on precipitation and temperature for Iran using RCP scenarios. *Journal of Water and Climate Change* **12** (1), 166–184.

Eamus, D. 1991 The interaction of rising CO_2 and temperatures with water use efficiency. *Plant, Cell & Environment* **14**, 843–852.

Ehteram, M., Mousavi, S. F., Karami, H., Farzin, S., Singh, V. P., Chau, K. W. & El-Shafie, A. 2018 Reservoir operation based on evolutionary algorithms and multi-criteria decision-making under climate change and uncertainty. *Journal of Hydroinformatics* **20** (2), 332–355.

Ficklin, D. L., Luedeling, E. & Zhang, M. 2010 Sensitivity of groundwater recharge under irrigated agriculture to changes in climate, CO_2 concentrations and canopy structure. *Agricultural Water Management* **97** (7), 1039–1050.

Field, C. B., Jackson, R. B. & Mooney, H. A. 1995 Stomatal responses to increased CO_2: implications from the plant to the global scale. *Plant, Cell & Environment* **18**, 1214–1225.

Foster, T., Brozović, N., Butler, A. P., Neale, C. M. U., Raes, D., Steduto, P., Fereres, E. & Hsiao, T. C. 2017 AquaCrop-OS: an open source version of FAO's crop water productivity model. *Agricultural Water Management* **181**, 18–22.

GEC 2009 *Ground Water Resource Estimation Methodology*. Report of the Ground Water Resource Estimation Committee, Ministry of Water Resources, Government of India, New Delhi, India. Available from: http://cgwb.gov.in/docum ents/gec97.pdf.

GEC 2017 *Detailed Guidelines for Implementing the Ground Water Resource Estimation Methodology 2015*. Central Ground Water Board, Ministry of Water Resources, Government of India, New Delhi, India. Available from: http://cgwb.gov.in/GW-Assessment/2020-11-17_Detailed_Guidelines_GEC2015.pdf.

Gobinath, M., Sahu, S. K., Ram, P. & Jhariya, D. C. 2022 Groundwater flow modeling study to assess the sustainability of groundwater resource in and around Bemetara Block, Chhattisgarh. India. *Journal of the Geologic Society of India* **98**, 712–719. https://doi.org/10.1007/s12594-022-2048-4.

Hamlet, A. F., Salathé, E. P. & Carrasco, P. 2010 Statistical downscaling techniques for global climate model simulations of temperature and precipitation with application to water resources planning studies. In: *Final Report for the Columbia Basin Climate Change Scenarios Project*, Climate Impacts Group, Center for Science in the Earth System, Joint Institute for the Study of the Atmosphere and Ocean, University of Washington, Seattle, WA, USA, ch. 4. https://doi.org/10.6069/bjoayxkb.

Harbaugh, A. W. 2005 *MODFLOW-2005. The US Geological Survey Modular Ground-Water Model – The Ground-Water Flow Process*. US Geological Survey Techniques and Methods 6-A16, US Geological Survey, Reston, VA, USA.

Hatfield, J. L. & Dold, C. 2019 Water-use efficiency: advances and challenges in a changing climate. *Frontiers in Plant Science* **10**, 103. https://doi.org/10.3389/fpls.2019.00103.

Hong, T., Dong, W., Ji, D., Dai, T., Yang, S. & Wei, T. 2019 The response of vegetation to rising CO_2 concentrations plays an important role in future changes in the hydrological cycle. *Theoretical and Applied Climatology* **136**, 135–144.

Hughes, N., Lu, M., Soh, W. Y. & Lawson, K. 2022 Modelling the effects of climate change on the profitability of Australian farms. *Climatic Change* **172**, 12. https://doi.org/10.1007/s10584-022-03356-5.

Hunt, R. J. & Feinstein, D. T. 2012 MODFLOW-NWT: robust handling of dry cells using a Newton formulation of MODFLOW-2005. *Groundwater* **50** (5), 659–663. https://doi.org/10.1111/j.1745-6584.2012.00976.x.

IPCC 2013 *Climate Change 2013: The Physical Science Basis. Contribution of Working Group I to the Fifth Assessment Report of the Intergovernmental Panel on Climate Change*. Cambridge University Press, Cambridge, UK and New York, NY, USA.

Islam, A., Ahuja, L. R., Garcia, L. A., Ma, L. & Saseendran, A. S. 2012a Modeling the effect of elevated CO_2 and climate change on potential evapotranspiration in the semi-arid Central Great Plains. *Transactions of the ASABE* **55** (6), 2135–2146. https://doi.org/10.13031/2013.42505.

Islam, A., Ahuja, L. R., Garcia, L. A., Ma, L., Saseendran, A. S. & Trout, T. J. 2012b Modeling the impacts of climate change on irrigated corn production in the Central Great Plains. *Agricultural Water Management* **110**, 94–108. https://doi.org/10.1016/j.agwat.2012.04.004.

Islam, A., Sikka, A. K., Saha, B. & Singh, A. 2012c Streamflow response to climate change in the Brahmani River basin, India. *Water Resources Management* **26**, 1409–1424. doi:10.1007_s11269-011-9965-0.

Jalota, S. K., Ray, S. S. & Panigrahy, S. 2009 Effects of elevated CO_2 and temperature on productivity of three main cropping systems in Punjab State of India: a simulation analysis. In: *ISPRS Archives XXXVIII-8/W3 Workshop Proceedings: Impact of Climate Change on Agriculture* (Panigrahy, S., Ray, S. S. & Parihar, J. S., eds), ISPRS WG VIII/6, Agriculture, Ecosystem and Bio-diversity SAC (ISRO), Ahmedabad, India, pp. 138–142.

Jones, N. L. 1999 *SEEP2D Primer*. Environmental Modeling Research Laboratory, Brigham Young University, Provo, UT, USA.

Kambale, J. B., Singh, D. K. & Sarangi, A. 2016 Impact of climate change on groundwater recharge in a semi-arid region of northern India. *Applied Ecology & Environmental Research* **15** (1), 335–362.

Khadri, S. F. R. & Pande, C. 2016 Ground water flow modeling for calibrating steady state using MODFLOW software: a case study of Mahesh River basin, India. *Modelling Earth System and Environment* **2**, 39. https://doi.org/10.1007/s40808-015-0049-7.

Kipp, K. L. 1997 *Guide to the Revised Heat and Solute Transport Simulator; HST3D, Version 2*. Water-Resources Investigations Report 97-4157, US Geological Survey, Denver, CO, USA. https://doi.org/10.3133/wri974157.

Kirschbaum, M. U. F. & McMillan, A. M. S. 2018 Warming and elevated CO_2 have opposing influences on transpiration. Which is more important? *Current Forestry Reports* **4**, 51–71.

Kulkarni, A., Sabin, T. P., Chowdary, J. S., Rao, K. K., Priya, P., Gandhi, N., Bhaskar, P., Buri, V. K., Sabade, S. S., Pai, D. S., Ashok, K., Mitra, A. K., Niyogi, D. & Rajeevan, M. 2020 Precipitation changes in India. In: *Assessment of Climate Change over the Indian Region* (Krishnan, R., Sanjay, J., Gnanaseelan, C., Mujumdar, M., Kulkarni, A. & Chakraborty, S., eds), Springer, Singapore, pp. 47–72. https://doi.org/10.1007/978-981-15-4327-2_3.

Kumar, C. P. 2019 An overview of commonly used groundwater modelling software. *International Journal of Advanced Research in Science, Engineering and Technology* **6** (1), 7854–7865.

Kumar, S., Narjary, B., Kumar, K., Jat, H. S., Kamra, S. K. & Yadav, R. K. 2019 Developing soil matric potential-based irrigation strategies of direct-seeded rice for improving yield and water productivity. *Agricultural Water Management* **215**, 8–15.

Kumar, S., Narjary, B., Nand, V., Islam, A., Yadav, R. K. & Kamra, S. K. 2022 Modeling climate change impact on groundwater and adaptation strategies for its sustainable management in the Karnal district of Northwest India. *Climatic Change* **173**, 3. https://doi.org/10.1007/s10584-022-03393-0.

Kundu, S., Khare, D. & Mondal, A. 2017 Future changes in rainfall, temperature and reference evapotranspiration in the central India by least square support vector machine. *Geoscience Frontiers* **8**, 583–596.

Langevin, C. D., Hughes, J. D., Banta, E. R., Niswonger, R. G., Panday, S. & Provost, A. M. 2017 *Documentation for the MODFLOW 6 Groundwater Flow (GWF) Model*. US Geological Survey Techniques and Methods, Book 6, A55, US Geological Survey, Reston, VA, USA. https://doi.org/10.3133/tm6A55.

Leipprand, A. & Gerten, D. 2006 Global effects of doubled atmospheric CO_2 content on evapotranspiration, soil moisture and runoff under potential natural vegetation. *Hydrological Sciences Journal* **51** (1), 171–185. https://doi.org/10.1623/hysj.51.1.171.

Lenka, N. K., Lenka, S., Thakur, J. K., Yashona, D. S., Shukla, A. K., Elanchezhian, R., Singh, K. K., Biswas, A. K. & Patra, A. K. 2020 Carbon dioxide and temperature elevation effects on crop evapotranspiration and water use efficiency in soybean as affected by different nitrogen levels. *Agricultural Water Management* **230**, 105936. https://doi.org/10.1016/j.agwat.2019.105936.

Lenka, N. K., Lenka, S., Yashona, D. S., Shukla, A. K., Elanchezhian, R., Dey, P., Agrawal, P. K., Biswas, A. K. & Patra, A. K. 2021 Carbon dioxide and/or temperature elevation effect on yield response, nutrient partitioning and use efficiency of applied nitrogen in wheat crop in central India. *Field Crops Research* **264**, 108084.

Liao, D., Niu, J., Kang, S., Singh, S. K. & Du, T. 2021 Effects of elevated CO_2 on the evapotranspiration over the agricultural land in Northwest China. *Journal of Hydrology* **593**, 125858. https://doi.org/10.1016/j.jhydrol.2020.125858.

Lin, H. C. J., Richards, D. R., Talbot, C. A., Yeh, G. T., Cheng, J. R., Cheng, H. P. & Jones, N. L. 1997 *FEMWATER: A Three-Dimensional Finite Element Computer Model for Simulating Density-Dependent Flow and Transport in Variably Saturated Media*, Technical Report CHL-97-12. US Army Corps of Engineers Waterways Experiment Station, Vicksburg, MS, USA.

Mali, S. S., Shirsath, P. B. & Islam, A. 2021 A high-resolution assessment of climate change impact on water footprints of cereal production in India. *Scientific Reports* **11**, 8715. https://doi.org/10.1038/s41598-021-88223-6.

McDonald, M. G. & Harbaugh, A. W. 1988 *A Modular Three-Dimensional Finite-Difference Ground-Water Flow Model*. Techniques of Water-Resources Investigations 6-A1, US, Geological Survey, Reston, VA, USA. https://doi.org/10.3133/twri06A1.

Minhas, P. S., Yadav, R. K., Lal, K. & Chaturvedi, R. K. 2015 Effect of long-term irrigation with wastewater on growth, biomass production and water use by Eucalyptus (*Eucalyptus tereticornis* Sm.) planted at variable stocking density. *Agricultural Water Management* **152**, 151–160.

Ministry of Agriculture 2013 *Crop Diversification Program in Haryana, Punjab & Western Uttar Pradesh*. Ministry of Agriculture (MoA), New Delhi, India.

Mndela, M., Tjelele, J. T., Madakadze, I. C., Mangwane, M., Samuels, I. M., Muller, F. & Pule, H. T. 2022 A global meta-analysis of woody plant responses to elevated CO_2: implications on biomass, growth, leaf N content, photosynthesis and water relations. *Ecological Processes* **11**, 52. https://doi.org/10.1186/s13717-022-00397-7.

Mohanty, S., Jha, M. K., Kumar, A. & Panda, D. K. 2013 Comparative evaluation of numerical model and artificial neural network for simulating groundwater flow in Kathajodi–Surua Inter-basin of Odisha, India. *Journal of Hydrology* **495**, 38–51.

Mohanty, M., Sinha, N. K., Hati, K. M., Reddy, K. S. & Chaudhary, R. S. 2015 Elevated temperature and carbon dioxide concentration effects on wheat productivity in Madhya Pradesh: a simulation study. *Journal of Agrometeorology* **17** (2), 185–189.

Morison, J. I. L., 1987 CO_2 concentration and stomatal response to CO_2 stomatal function. In: *Stomatal Function* (Zeiger, E., Farquhar, G. D. & Cowan, I. R., eds.), Stanford University Press, Stanford, CA, USA, pp. 229–251.

Nand, V., Neha, Kumar, S., Narjary, B., Dash, S. S., Yadav, G., Yadav, R. K. & Malik, A. 2021 Effects of rising temperature and CO_2 concentration on reference evapotranspiration and identification of significant governing meteorological variables in a semi-arid irrigated region. *Journal of Agricultural Mechanization in Asia, Africa Latin America* **52**, 2893–2906.

Narjary, B., Kumar, S., Meena, M. D., Kamra, S. K. & Sharma, D. K. 2021 Effects of shallow saline groundwater table depth and evaporative flux on soil salinity dynamics using Hydrus-1D. *Agricultural Research* **10**, 105–115. https://doi.org/10.1007/s40003-020-00484-1.

Niu, J., Sivakumar, B. & Chen, J. 2013 Impacts of increased CO_2 on the hydrologic response over the Xijiang (West River) basin, South China. *Journal of Hydrology* **505**, 218–227.

O'Grady, A. P., Tissue, D. T. & Beadle, C. L. 2011 Canopy processes in a changing climate. *Tree Physiology* **31** (9), 887–892.

Pandey, V., Sharma, M., Deeba, F., Maurya, V. K., Gupta, S. K., Singh, S. P., Mishra, A. & Nautiyal, C. S. 2017 Impact of elevated CO_2 on wheat growth and yield under free air CO_2 enrichment. *American Journal of Climate Change* **6**, 573–596.

Pollock, D. W. 2016 *User Guide for MODPATH Version 7 – A Particle-Tracking Model for MODFLOW*. US Geological Survey Open-File Report 2016-1086, US Geological Survey, Reston, VA, USA. http://dx.doi.org/10.3133/ofr20161086.

Priya, A., Nema, A. K. & Islam, A. 2014 Effect of climate change and elevated CO_2 on reference evapotranspiration in Varanasi, India: a case study. *Journal of Agrometeorology* **16** (1), 44–51. https://doi.org/10.54386/jam.v16i1.1485.

Qu, C. H., Li, X. X., Jiu, H. & Liu, Q. 2019 The impacts of climate change on wheat yield in the Huang-Huai-Hai Plain of China using DSSAT-CERES-Wheat model under different climate scenarios. *Journal of Integrative Agriculture* **18** (6), 1379–1391.

Raes, D., Steduto, P., Hsiao, T. C. & Fereres, E. 2022 Chapter 3: Calculation procedures. In: *AquaCrop Version 7.0 Reference Manual*, Food and Agriculture Organization of the United Nations, Rome, Italy.

Reinecke, R., Schmied, H. M., Trautmann, T., Andersen, L. S., Burek, P., Flörke, M., Gosling, S. N., Grillakis, M., Hanasaki, N., Koutroulis, A., Pokhrel, Y., Thiery, W., Wada, Y., Yusuke, S. & Döll, P. 2021 Uncertainty of simulated groundwater recharge at different global warming levels: a global-scale multi-model ensemble study. *Hydrology and Earth System Sciences* **25**, 787–810.

Rossman, N. R. & Zlotnik, V. A. 2013 Review: Regional groundwater flow modeling in heavily irrigated basins of selected states in the western United States. *Hydrogeology Journal* **21**, 1173–1192. doi:10.1007/s10040-013-1010-3.

Rumbaugh, J. O. & Rumbaugh, D. B. 2017 *Guide to Using Groundwater Vistas Version 7*. Environmental Simulations, Inc., Leesport, PA, USA.

Sahoo, S. & Jha, M. K. 2017 Numerical groundwater-flow modeling to evaluate potential effects of pumping and recharge: implications for sustainable groundwater management in the Mahanadi delta region, India. *Hydrogeology Journal* **25**, 2489–2511. https://doi.org/10.1007/s10040-017-1610-4.

Sanjay, J., Revadekar, J. V., Ramarao, M. V. S., Borgaonkar, H., Sengupta, S., Kothawale, D. R., Patel, J., Mahesh, R., Ingle, S., AchutaRao, K., Srivastava, A. K. & Ratnam, J. V. 2020 Temperature changes in India. In: *Assessment of Climate Change over the Indian Region* (Krishnan, R., Sanjay, J., Gnanaseelan, C., Mujumdar, M., Kulkarni, A. & Chakraborty, S., eds), Springer, Singapore, pp. 21–45. https://doi.org/10.1007/978-981-15-4327-2_2.

Savabi, M. R. & Stockle, C. O. 2001 Modeling the possible impact of increased CO_2 and temperature on soil water balance, crop yield, and soil erosion. *Environmental Modelling & Software* **16**, 631–640. https://doi.org/10.1016/S1364-8152(01)00038-X.

Shaban, A. & Sharma, R. N. 2007 Water consumption patterns in domestic households in major cities. *Economic and Political Weekly* **42** (23), 2190–2197.

Shimono, H., Nakamura, H., Hasegawa, T. & Okada, M. 2013 Lower responsiveness of canopy evapotranspiration rate than of leaf stomatal conductance to open-air CO_2 elevation in rice. *Global Change Biology* **19**, 2444–2453. https://doi.org/10.1111/gcb.12214.

Šimůnek, J., Šejna, M., Brunetti, G. & van Genuchten, M. T. 2022 *The HYDRUS Software Package for Simulating the One-, Two-, and Three-Dimensional Movement of Water, Heat, and Multiple Solutes in Variably-Saturated Porous Media, Technical Manual I, Hydrus 1D, Version 5.x*. PC Progress, Prague, Czech Republic.

Sonali, P., Kumar, N. D. & Nanjundiah, R. S. 2017 Intercomparison of CMIP5 and CMIP3 simulations of the 20th-century maximum and minimum temperatures over India and detection of climatic trends. *Theoretical and Applied Climatology* **128**, 465–489.

Steduto, P., Hsiao, T. C., Fereres, E. & Raes, D. 2012 *Crop Yield Response to Water*. FAO Irrigation and Drainage Paper 66, Food and Agriculture Organization of the United Nations, Rome, Italy. Available from: https://www.fao.org/3/i2800e/i2800e.pdf.

Tohver, I. M., Hamlet, A. F. & Lee, S. Y. 2014 Impacts of 21st-century climate change on hydrologic extremes in the Pacific Northwest region of North America. *Journal of American Water Resources Association* **50**, 1461–1476.

Trescott, P. C. 1975 *Documentation of Finite Difference Model for Simulation of Three-Dimensional Ground-Water Flow*. US Geological Survey Open-File Report 75-438, US Geological Survey, Reston, VA, USA. https://doi.org/10.3133/ofr75438.

van Ittersum, M. K., Howden, S. M. & Asseng, S. 2003 Sensitivity of productivity and deep drainage of wheat cropping systems in a Mediterranean environment to changes in CO_2, temperature and precipitation. *Agriculture, Ecosystems & Environment* **97** (1–3), 255–273.

Voss, C. I. & Provost, A. M. 2002 *SUTRA: A Model for Saturated-Unsaturated Variable-Density Ground-Water Flow with Solute or Energy Transport*. US Geological Survey Water-Resources Investigations Report 02-4231, US Geological Survey, Reston, VA, USA.

Waterloo Hydrogeologic. 2019 *Visual MODFLOW Flex 6.1: Integrated Conceptual & Numerical Groundwater Modeling Software*. Waterloo ON, Hydrogeologic, Inc., Waterloo, Canada.

Wood, A. W., Maurer, E. P., Kumar, A. & Lettenmaier, D. P. 2002 Long-range experimental hydrologic forecasting for the eastern United States. *Journal of Geophysical Research* **107** (D20), 4429.

Xiao, D., Liu, D. L., Wang, B., Feng, P., Bai, H. & Tang, J. 2020 Climate change impact on yields and water use of wheat and maize in the North China Plain under future climate change scenarios. *Agricultural Water Management* **238**, 106238.

Xing, H. M., Xu, X. G., Li, Z. H., Chen, Y. J., Feng, H. K., Yang, G. J. & Chen, Z. X. 2017 Global sensitivity analysis of the AquaCrop model for winter wheat under different water treatments based on the extended Fourier amplitude sensitivity test. *Journal of Integrative Agriculture* **16** (11), 2444–2458.

Xu, J., Bai, W., Li, Y., Wang, H., Yang, S. & Wei, Z. 2019 Modeling rice development and field water balance using AquaCrop model under drying-wetting cycle condition in eastern China. *Agricultural Water Management* **213**, 289–297.

Yang, C. & Lei, H. M. 2022 Climate and management impacts on crop growth and evapotranspiration in the North China Plain based on long-term eddy covariance observation. *Agricultural and Forest Meteorology* **325**, 109147. https://doi.org/10.1016/j.agrformet.2022.109147.

Zhang, Q., Shen, Z., Xu, C. Y., Sun, P., Hu, P. & He, C. 2019 A new statistical downscaling approach for global evaluation of the CMIP5 precipitation outputs: model development and application. *Science of the Total Environment* **690**, 1048–1067.

Zhou, Y. & Li, W. 2011 A review of regional groundwater flow modelling. *Geoscience Frontiers* **2** (2), 205–214. doi:10.1016/j.gsf.2011.03.003.

First received 18 January 2023; accepted in revised form 30 May 2023. Available online 8 June 2023